

## Creep and Relaxation Dynamics of Domain Walls in Periodically Poled $\text{KTiOPO}_4$

Th. Braun,<sup>1</sup> W. Kleemann,<sup>1,\*</sup> J. Dec,<sup>1,2</sup> and P. A. Thomas<sup>3</sup>

<sup>1</sup>Angewandte Physik, Universität Duisburg-Essen, D-47048 Duisburg, Germany

<sup>2</sup>Institute of Physics, University of Silesia, PL 40-480 Katowice, Poland

<sup>3</sup>Department of Physics, University of Warwick, Warwick, United Kingdom

(Received 26 October 2004; published 24 March 2005)

Creep and relaxation of domain walls under ac electric fields are observed in an ideal model system, periodically poled  $\text{KTiOPO}_4$ , to occur in different regimes, which are separated by dynamic phase transitions at frequencies  $f_m(T) = f_{m0} \exp(-\Delta E/k_B T)$ , with  $f_{m0} = 3 \times 10^9$  Hz and  $\Delta E = 0.6$  eV. Power law dispersion of the creep susceptibility,  $\chi \propto 1 + (i\omega\tau)^{-\beta}$ , with  $\beta \approx 0.4$ , and large nonlinearity encountered at  $f < f_m$ , is contrasted with Cole-Cole-type relaxational dispersion,  $\chi \propto (1 + [i\omega\tau]^{1-\alpha})^{-1}$ , with  $\alpha \approx 0.3$ , at  $f > f_m$ .

DOI: 10.1103/PhysRevLett.94.117601

PACS numbers: 77.22.Gm, 77.80.Dj, 77.84.Dy, 78.30.Ly

Quenched randomness in ferroic systems (ferroelectrics, ferromagnets) containing domain walls (DWs) has interesting consequences on its response to an external conjugate field. Depending on the strength of the driving field,  $h$ , the DWs exhibit different states of motion below and above a critical “depinning” field,  $h_c$ , which separates the regions of thermally activated creep and friction-limited slide, respectively [1]. These stationary states of motion have only recently been observed to comply perfectly with theory on well-defined DWs both in ferromagnetic [2] and ferroelectric [3] systems driven by external dc fields. In contrast, information on the complementary vibrating DW states excited by external ac fields is still very limited. In this Letter a periodically poled ferroelectric single crystal of  $\text{KTiOPO}_4$  (KTP) with planar DWs is presented as an ideal system revealing an additional state of motion at high frequencies, which does not occur in the stationary dc limit. This polydispersive relaxation mode [4] converts into mesoscopic creep of DW segments via a dynamic phase transition below a critical frequency  $f_m$  under weak field amplitudes  $h_0$ .

The dynamic behavior of DWs driven in a random medium by a periodic external field  $h = h_0 \exp(i\omega t)$  can be modeled by considering one planar interface  $z(x, t)$  in a quenched random field  $h_r(x, z)$  obeying the “quenched Edwards-Wilkinson equation” [5,6],

$$\gamma^{-1}(\partial z/\partial t) = \Gamma \nabla^2 z + h_0 \exp(i\omega t) + h_r(x, z), \quad (1)$$

where  $\gamma$  and  $\Gamma$  are the mobility and the stiffness constant, respectively. The cycles of the integrated electric or magnetic polarization,  $\eta$  ( $\equiv P$  or  $M$ , respectively) vs  $h$ , depend crucially on temperature  $T$ , angular frequency,  $\omega = 2\pi f$ , and ac field amplitude,  $h_0$  ( $\equiv E_0$  or  $B_0$ , respectively). As a function of these parameters, they are expected to undergo dynamical phase transitions, whenever the dynamic order parameter  $Q = (\omega/2\pi) \oint \eta dt$  changes as  $Q = \eta_0 \leftrightarrow Q \neq \eta_0$  with a discontinuity of  $\partial Q/\partial h$  (or  $\partial Q/\partial f$ ) [7]. When increasing  $h_0$ , the cycles  $\eta$  vs  $h$  are expected to pass through four regimes. First, at very low fields,  $h_0 < h_\omega$ ,

only local “relaxation,” but no macroscopic motion of the DWs occurs at finite frequencies,  $\omega > 0$ . This is shown in the schematic  $\eta$  vs  $h$  diagram of Fig. 1(a) by a horizontal double arrow with  $Q = \eta_0$  denoted as 1 on the level of the remanent polarization. Second, within the range  $h_\omega < h_0 < h_1$ , thermally activated drift motion (“creep”) with a smaller value,  $Q < \eta_0$  is expected [Fig. 1(a), loop 2]. A dynamic *relaxation-to-creep* transition will occur, if  $\partial Q/\partial h$  (or  $\partial Q/\partial f$ ) shows a discontinuity at  $h_\omega$  for constant  $f$  (or at  $f_m$  for constant  $h_0$ ; see discussion below).  $Q = \eta_0$  denotes DWs relaxing between local minima of the potential landscape, while they move thermally activated over global potential barriers in the case  $Q < \eta_0$ . When increasing the amplitude beyond the depinning threshold,  $h_1$  ( $\approx$  coercive field), the “sliding” regime is encountered within  $h_1 < h_0 < h_2$ . Here the hysteresis loop becomes larger but is still acentric,  $Q \neq 0$  [Fig. 1(a), loop 3]. As the *creep-to-slide* transition under constant field conditions is sharp only at  $T = 0$  [8], this also applies to the dynamic “transition,” where  $Q$  varies smoothly. Finally, for  $h_0 > h_2$ , a complete reversal of the polarization (“switching”) occurs in the whole sample in each half period,  $T/2 = \pi/\omega$ . Owing to the centric hysteresis loop with  $Q = 0$  [Fig. 1(a), loop 4], one expects again a dynamic transition, the *slide-to-switch* transition.

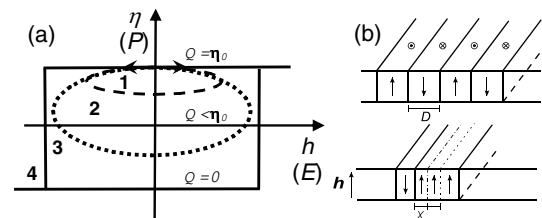


FIG. 1. (a) Schematic sketch of order parameter cycles  $\eta(h)$  of a ferroic and  $P(E)$  of a ferroelectric system, respectively, for different ac field amplitudes (see text). (b),(c) Ferroic stripe domain pattern with perpendicular anisotropy in zero and non-zero external field, respectively (see text).

Since all transition fields,  $h_\omega$ ,  $h_1$ , and  $h_2$ , depend strongly on both  $T$  and  $\omega$  [6], a series of dynamic phase transitions emerges in the  $T - \omega - h$  parameter space, part of which has recently been observed in quite different domain state systems. We have considered the strongly disordered uniaxial “relaxor” ferroelectric  $\text{Sr}_{1-x}\text{Ba}_x\text{Nb}_2\text{O}_6$  (SBN) [9], the nanoparticulate ferromagnetic “discontinuous metal-insulator multilayer”  $[\text{Co}_{80}\text{Fe}_{20}(1.4 \text{ nm})/\text{Al}_2\text{O}_3(3 \text{ nm})]_{10}$  (DMIM) [10], and the isotope exchanged “quantum ferroelectric”  $\text{SrTi}^{18}\text{O}_3$  (STO18) [11]. Universal features are encountered: (i) *Relaxation* spectra at high frequency, weak field, and/or low temperature appear essentially white noiselike in all systems [9–11]; (ii) *creep* spectra at intermediate frequency, field, and/or temperature, which exhibit power law dispersion

$$\chi(\omega) = \chi_\infty(1 + [i\omega\tau]^{-\beta}), \quad 0 < \beta < 1. \quad (2)$$

The exponent  $\beta$  was introduced semiempirically within an adiabatic response theory based on field-induced sideways DW motion [9]. Its deviation from ideal conductivity,  $\beta = 1$ , was attributed to the nonlinear dependence of the creep velocity on the applied field  $h$ ,  $v \propto \exp[-\alpha(h_1/h)^\delta]$ , where  $\alpha$ ,  $h_1$ , and  $\delta$  are constants [1]. (iii) *Slide* spectra at low frequency, strong field, and/or high temperature come close to the ideal case  $\beta = 1$  in DMIM [10] and STO18 [11]. (iv) *Switching* spectra mimicked by a monodispersive Debye process,

$$\chi(\omega) = \chi_\infty(1 + i\omega\tau)^{-1}, \quad (3)$$

were observed at very low frequency, strong field, and/or high temperature in DMIM [10].

The theory developed for the time domain [6] has recently been transferred into the frequency domain either by integrating Eq. (1) [12] or by considering scaling properties and a broad distribution of effective DW mobilities,  $\mu(h)$  [13]. However, none of the experimental systems investigated so far has the simple domain structure of the idealized models [6,9,12,13]. All of them, DMIM [10], SBN [14], and STO18 [15], are random field systems with a wide size distribution of fractal domains, whose dynamic properties are not necessarily expected to comply with single DW theories. Probably for this reason, the spectral character of the DW relaxation spectra has not been clarified yet. This shortcoming is remedied in this Letter, which presents data on an *ideal system* represented by the regular domain state of a periodically poled crystal of ferroelectric KTP (PPKTP), which is weakly disordered due to cationic superionicity [16]. Its dielectric susceptibility spectra due to DW motion show distinct frequency ranges for relaxation and creep with Arrhenius activated dynamic phase transitions. The relaxation is of the polydispersive Cole-Cole type similarly as found, e.g., in the relaxor lanthanum lead zirconate titanate [17].

The PPKTP sample used in this work has a domain width  $D = 4.5 \mu\text{m}$ , as shown schematically in Fig. 1(b). Periodic poling (period  $\Lambda = 9 \mu\text{m}$ ) was achieved with

standard lithographic methods described elsewhere [18]. Dielectric susceptibility data,  $\chi = \chi' - i\chi''$ , were measured on a parallel epiped-shaped PPKTP crystal (dimensions  $a = 5.5$ ,  $b = 6.0$ , and  $c = 0.58 \text{ mm}$ ) with a Solartron 1260 impedance analyzer via a 1296 dielectric interface. Gold electrodes were sputtered on the large  $c$  faces and covered with silver paint. Weak electric field amplitudes ( $E_0 = 175 \text{ V/m}$  for linear and up to  $5 \text{ kV/m}$  for nonlinear response) with frequencies  $10^{-4} < f < 10^7 \text{ Hz}$  were applied along the polar  $c$  axis, thus giving rise to periodic sideways motion of the DWs by distances  $x$  as indicated (largely exaggerated) in Fig. 1(c). Constant sample temperatures,  $190 \text{ K} < T < 390 \text{ K}$ , were stabilized to within  $\pm 0.05 \text{ K}$  in a self-built heating or cooling stage by a Lake Shore 340 temperature controller. In order to extract the DW contribution of the susceptibility, the background susceptibility of single domained KTP had to be subtracted from that of the PPKTP sample. It was prepared from the PPKTP sample by pulsed uniform poling (duration  $\Delta t \approx 2 \text{ s}$ ) along the polar  $c$  axis with an electric field of  $7 \text{ MV/m}$  at  $T = 233 \text{ K}$  while immersing the sample in an oil bath in order to avoid electrical breakdown. Since bulk KTP is a superionic conductor at  $T \geq 170 \text{ K}$  with a large intrinsic conductivity and considerable frequency dispersion [16,19], both sets of measurements were done under strictly identical conditions of temperature and field.

Figure 2 shows the difference spectra  $\Delta\chi'$  and  $\Delta\chi''$  (open and solid symbols, respectively) vs frequency,  $\log f$ , recorded with  $E_0 = 175 \text{ kV/m}$  at  $T = 190, 233, 323$ , and  $383 \text{ K}$ . In addition,  $\Delta\chi''(f, T = 283 \text{ K})$  is shown for three larger field amplitudes (see below). It is seen that all of the spectra consist of two subspectra, which are nearly distinct at low temperatures. The high- $f$  parts are of broadened Debye-type (bell-type  $\Delta\chi''$  spectra with  $\text{FWHM} \approx 2$  frequency decades; dispersion steps of  $\Delta\chi'$

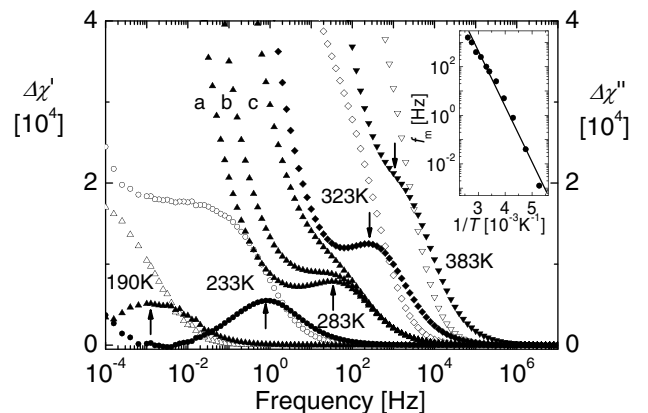


FIG. 2. ac susceptibility spectra  $\Delta\chi'$  and  $\Delta\chi''$  vs  $f$  (open and solid symbols, respectively) of planar DWs in PPKTP measured with  $E_0 = 175 \text{ V/m}$  at  $T = 190, 233, 323$ , and  $383 \text{ K}$ .  $\Delta\chi''$  vs  $f$  at  $T = 283 \text{ K}$  is shown for  $E_0 = 0.5$  (a),  $1.6$  (b), and  $5.2 \text{ kV/m}$  (c). The inset shows the peak frequencies  $f_m$  of  $\Delta\chi''(f)$  taken from this figure (arrows) and Fig. 3, plotted as  $\log f_m$  vs  $1/T$  together with a best-fitted Arrhenius line.

with height  $\approx 3\Delta\chi''_{\max}$ ), while the low- $f$  subspectra are inverse power-law-like for both  $\Delta\chi'$  and  $\Delta\chi''$ . With increasing  $T$  the peak frequency,  $f_m$ , of the high- $f$  loss spectrum shifts to higher values, as depicted by a plot of  $\log f_m$  vs  $1/T$  in the inset of Fig. 2. At  $T > 323$  K,  $f_m$  was determined by graphic decomposition. The best-fitted line evidences Arrhenius-type activation,  $f_m(T) = f_{m0} \times \exp(-\Delta E/k_B T)$ , with  $f_{m0} = (2.6 \pm 0.5) \times 10^9$  Hz and an average activation energy  $\Delta E = (0.60 \pm 0.03)$  eV. The observed weak decrease of  $\Delta E$  upon heating (Fig. 2, inset) is probably due to forced depinning of the DWs by increasingly mobile superionic carriers.

Figure 3 shows all of our data  $\Delta\chi'$  (a) and  $\Delta\chi''$  (b) vs  $f$  registered at  $T = 383$  (1), 363 (2), 343 (3), 323 (4), 303 (5), 293 (6), 273 (7), 253 (8), 233 (9), 210 (10), and 190 K (11). Since they vary over many decades between  $\approx 10^{-2}$  (high  $f$ ) and  $\approx 10^7$  (low  $f$ ), log-log plots are in order. Again it is seen that each individual spectrum contains two partial spectra, which monotonically decrease in a linear fashion at increasing  $f$ , thus showing inverse power law behavior,  $\propto f^{-\beta}$ . Also the peaks of  $\Delta\chi''$  (see Fig. 2) are visible—logarithmically compressed—between the steep high- $f$  and flat low- $f$  partial spectra. The particularly deep intermediate minimum found for  $T = 233$  K (curve 9) at  $f \approx 3$  mHz is marked by an arrow.

The polydispersive relaxation of the high- $f$  spectra is readily confirmed by Cole-Cole-type plots,  $\Delta\chi''$  vs  $\Delta\chi'$ , in Fig. 4. At low  $T$  the high- $f$  data (Fig. 4, lower left corner

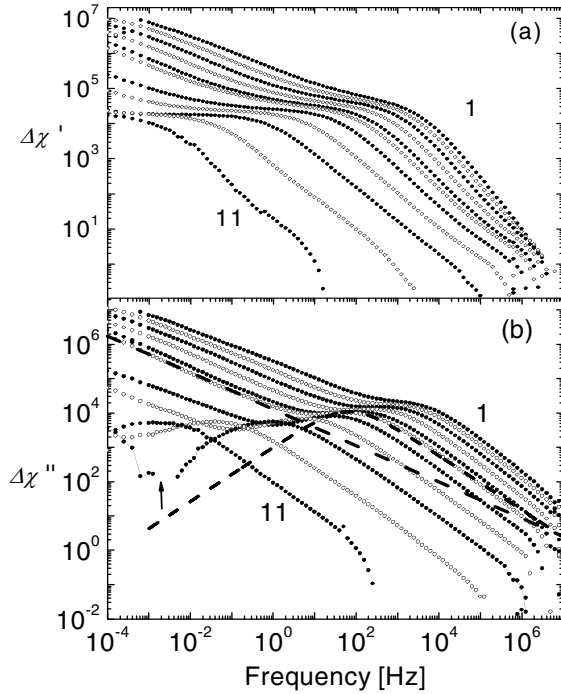


FIG. 3. Double logarithmic plot of ac susceptibility spectra  $\Delta\chi'$  (a) and  $\Delta\chi''$  (b) vs  $f$  registered at  $T = 383$  (1), 363 (2), 343 (3), 323 (4), 303 (5), 293 (6), 273 (7), 253 (8), 233 (9; minimum marked by an arrow), 210 (10), and 190 K (11). The data sets (6) are best fitted to Eqs. (2) and (4) by the broken lines.

and inset) form flattened semicircles, which are well described by Cole-Cole dispersion [20],

$$\Delta\chi(\omega) = \Delta\chi_{\infty} + (\Delta\chi'_s - \Delta\chi_{\infty}) / (1 + [i\omega\tau]^{1-\alpha}), \quad (4)$$

$$0 < \alpha < 1.$$

A best fit of the  $T = 233$  K data (curve 9) to the corresponding Cole-Cole function  $\Delta\chi''(\Delta\chi')$  [21] yields  $\Delta\chi'_s = 17820 \pm 65$ ,  $\chi_{\infty} \approx 0$ , and  $\alpha = 0.28 \pm 0.02$  (solid half circle). At low frequencies when approaching the static limit  $\Delta\chi'_s$ , the data sharply bend up into a monotonically rising line, which is well described by Eq. (2) [9],

$$\Delta\chi''(\omega) = \tan(\pi\beta/2)(\Delta\chi' - \Delta\chi'_s), \quad 0 < \beta < 1. \quad (5)$$

For the low- $f$  data of curve 9, we find  $\beta = 0.35 \pm 0.02$  (solid line) and  $\Delta\chi'_s = 17904 \pm 60$ , which corresponds to the high- $f$  cutoff of this type of response and coincides within errors with the above static limit. Closer inspection of the data shows that the exponent  $\beta$  slightly decreases on heating, thus indicating increasing disorder as expected for a superionic system.

At  $T \neq 233$  K, the *relaxation-to-creep transition* becomes slightly smeared (see inset of Fig. 4 for  $T = 210$  and 253 K), but even at  $T = 383$  K (Fig. 4, curve 1), both spectral features are still clearly distinguished. Exemplarily, the decomposition of  $\Delta\chi''(f)$  into the functions Eqs. (2) and (4) is shown for the data set (6) for  $T = 293$  K in Fig. 3(b). It has to be stressed, however, that the unprecedentedly sharp separation observed at  $T = 233$  K does not define a “critical” temperature. It rather results from different thermal shifts of the subspectra shown in Fig. 3. Their Arrhenius activated frequencies  $f(T) = f_0 \exp(-\Delta E/k_B T)$  associated with a fixed value of  $\Delta\chi''$  reveal different activation energies,  $\Delta E \approx 0.65$  (low  $f$ ) and 0.50 eV (high  $f$ ), since the average DW displacement in the

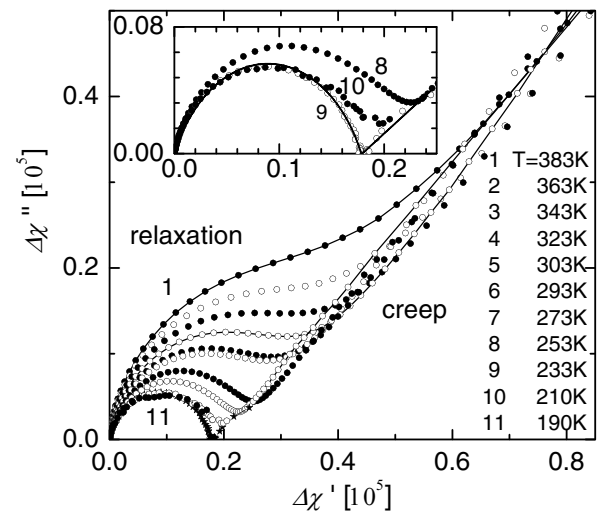


FIG. 4. Cole-Cole plots  $\Delta\chi''$  vs  $\Delta\chi'$  of the data in Fig. 3, partly connected by eye-guiding lines. Inset: Expanded plots of data sets (8)–(10) and best fits (solid lines) of Eqs. (2) and (4) to data set (9).

creep motion is determined by the highest energy barrier  $\Delta E_{\max}$ , while the relaxational response averages over all barrier heights thus probing  $\Delta E_{\text{av}} < \Delta E_{\max}$ . As a consequence, in Fig. 3(b) the creep spectra shift more rapidly at increasing  $T$  than the relaxation spectra. Hence, upon heating the creep branches approach the relaxation spectra and reduce the gap between them, which is widest at low  $T$ .

The transitionlike change from creep to relaxation does not involve overlap of both spectral functions. If the low- $f$  creep lines (as presented in Fig. 3) were extrapolated to high frequencies, they would readily cross the steep high- $f$  lines and thus bend up both the  $\Delta\chi'$  and  $\Delta\chi''$  vs  $f$  spectra at high frequencies. This is actually not observed in experiments. Hence, a correct description of the spectra has to use Eqs. (2) and (4) separately in their different ranges of validity.

Another criterion distinguishing the dynamic phases refers to their different dielectric nonlinearity. Figure 2 shows three  $\Delta\chi''$  vs  $f$  spectra taken at  $T = 283$  K with  $E_0 = 0.5, 1.7,$  and  $5.2$  kV/m. While they are essentially dispersion-free for  $f > f_m = 32$  Hz (arrow), they reveal considerable splitting in the low- $f$  region,  $f < f_m$ . This is attributed to the nonlinear increase of the DW velocity at increasing driving field [1], such that  $\Delta\chi = \epsilon_0^{-1} \langle dP/dE \rangle$  also increases with increasing amplitude. Our data comply well with a linear approximation,  $\Delta\chi'' = \Delta\chi''_0 + \Delta\chi''_1 E_0$ . On the other hand, the relaxation at high  $f$  is by nature linear in moderate fields, as long as the DW is locally captured in one valley [13]. Hence, the splitting of the response spectra is another indicator of the relaxation-to-creep transition.

As seen in Fig. 2 the nonlinear splitting starts gradually above the peak frequency,  $f_m$ , as expected in view of the different dynamic heterogeneities of the states involved. While the creep mode is controlled by the distribution function of DW mobilities, relaxation rather accounts for the distribution function of local double well potentials. Both functions cannot be identical. Hence, the relaxation-to-creep transition as defined by the frequency  $f_m(T, E_0)$  (see Fig. 2, inset) is probably smeared at any finite temperature. Interestingly, at zero temperature the creep regime shrinks to the dc limit,  $f \leq \lim_{T \rightarrow 0} f_m(T) = 0$ , where its response vanishes provided that  $h_0 < h_1$ . Simultaneously, also the relaxation spectrum, Eq. (4), shrinks to zero (see Fig. 4), since  $\lim_{T \rightarrow 0} \Delta\chi'_s(T) = 0$ .

In conclusion, we have shown that PPKTP is an ideal model system for demonstrating the dynamic phase transition on the frequency scale between creep and relaxation modes of ferroelectric DWs. Owing to the large aspect ratio between DW spacing and field-induced displacements, DW interactions may be neglected and an effective single DW theory seems justified. Since both modes are thermally activated, their spectra shrink to the singular point  $f = 0$  as  $T \rightarrow 0$ . Apart from this interesting low- $T$

regime, it will also be worth exploring the field dependence, which was shown to shift the phase boundary  $f_m$  vs  $T$  of the magnetic DMIM system to higher frequencies as  $h_0$  increases [10]. Probing the periodic motion of the DWs in PPKTP with piezoresponse force microscopy is another challenge.

This work was supported by Deutsche Forschungsgemeinschaft (DFG) within the framework of the Schwerpunktprogramm "Strukturgradienten in Kristallen" and by funding from the Engineering and Physical Sciences Research Council (EPSRC) of the U.K.

\*Electronic address: kleemann@uni-duisburg.de

- [1] M. V. Feigel'man, V. B. Geshkenbein, A. I. Larkin, and V. M. Vinokur, Phys. Rev. Lett. **63**, 2303 (1989).
- [2] S. Lemerle *et al.*, Phys. Rev. Lett. **80**, 849 (1998).
- [3] T. Tybell, P. Paruch, T. Giamarchi, and J.-M. Triscone, Phys. Rev. Lett. **89**, 097601 (2002).
- [4] T. Nattermann, Y. Shapir, and I. Vilfan, Phys. Rev. B **42**, 8577 (1990).
- [5] S. F. Edwards and D. Wilkinson, Proc. R. Soc. London A **381**, 17 (1982).
- [6] T. Nattermann, V. Pokrovsky, and V. M. Vinokur, Phys. Rev. Lett. **87**, 197005 (2001); A. Glatz, T. Nattermann, and V. Pokrovsky, *ibid.* **90**, 047201 (2003).
- [7] B. K. Chakrabarti and M. Acharyya, Rev. Mod. Phys. **71**, 847 (1999).
- [8] P. Chauve, T. Giamarchi, and P. Le Doussal, Phys. Rev. B **62**, 6241 (2000).
- [9] W. Kleemann, J. Dec, S. Miga, and R. Pankrath, Phys. Rev. B **65**, 220101(R) (2002).
- [10] X. Chen *et al.*, Phys. Rev. Lett. **89**, 137203 (2002).
- [11] J. Dec, W. Kleemann, and M. Itoh, Ferroelectrics **298**, 163 (2004).
- [12] O. Petracic, A. Glatz, and W. Kleemann, Phys. Rev. B **70**, 214432 (2004).
- [13] A. A. Fedorenko, V. Mueller, and S. Stepanow, Phys. Rev. B **70**, 224104 (2004).
- [14] W. Kleemann *et al.*, Europhys. Lett. **57**, 14 (2002).
- [15] L. Zhang *et al.*, Eur. Phys. J. B **28**, 163 (2002).
- [16] Q. Jiang *et al.*, Phys. Rev. B **66**, 094102 (2002).
- [17] S. Kamba *et al.*, J. Phys. Condens. Matter **12**, 497 (2000).
- [18] G. Rosenman and A. Skilar, Appl. Phys. Lett. **73**, 3650 (1998).
- [19] The ac susceptibility data taken on the bulk single domain KTP crystal (to be published elsewhere) resemble the DW spectra in that they also show low- $f$  inverse power law dispersion,  $\chi(\omega) \propto (1 + [i\omega\tau]^{-\beta})$ , due to variable range hopping in the superionic state [T. Ishii, Prog. Theor. Phys. **73**, 1084 (1985)]. Although this contribution to the total electric response is about 1 order of magnitude smaller than the DW contribution, it is highly probable that the observed DW pinning is partly due to the superionic disorder.
- [20] K. S. Cole and R. H. Cole, J. Chem. Phys. **9**, 341 (1941).
- [21] M. Hagiwara, J. Magn. Magn. Mater. **177-181**, 89 (1998).